Polymer(Korea), Vol. 37, No. 3, pp. 332-341
http://dx.doi.org/10.7317/pk.2013.37.3.332

ISSN 0379-153X(Print)
ISSN 2234-8077(Online)

H-형태 양친매성 펜타블록 공중합체의 화학효소적 합성과 자기회합거동 평가

Peng Chen, Ya-Peng Li†, Cai-Jin Li, Xin-Lei Meng, Bao Zhang*, Ming Zhu,
Yan-Jing Liu**, and Jing-Yuan Wang

Alan G. MacDiarmid Institute, College of Chemistry, Jilin University, Changchun 130012, China
*Changchun Institute of Applied Chemistry Chinese Academy of Sciences, Changchun 130022, China
**The Affiliated hospital, Changchun University of Chinese Medicine, Changchun 130021, China

(2012년 10월 23일 접수, 2012년 12월 24일 수정, 2013년 1월 8일 채택)

Chemoenzymatic Synthesis of H-shaped Amphiphilic Pentablock Copolymer and Its Self-assembly Behavior

Peng Chen, Ya-Peng Li†, Cai-Jin Li, Xin-Lei Meng, Bao Zhang*, Ming Zhu, Yan-Jing Liu, and Jing-Yuan Wang**

Alan G. MacDiarmid Institute, College of Chemistry, Jilin University, Changchun 130012, China
**Changchun Institute of Applied Chemistry Chinese Academy of Sciences, Changchun 130022, China*
***The Affiliated hospital, Changchun University of Chinese Medicine, Changchun 130021, China*

(Received October 23, 2012; Revised December 24, 2012; Accepted January 8, 2013)

Abstract: H-shaped amphiphilic pentablock copolymers $(PSt)_2$-*b*-PCL-*b*-PEO-*b*-PCL-*b*-$(PSt)_2$ was synthesized via chemoenzymatic method by combining enzyme-catalyzed ring-opening polymerization (eROP) of ε-caprolactone (ε-CL) and atom transfer radical polymerization (ATRP) of styrene. By this process, we obtained copolymers with controlled molecular weight and low polydispersity. The structure and composition of the obtained copolymers were characterized by nuclear magnetic resonance (NMR), gel permeation chromatography (GPC) and infrared spectroscopy analysis (IR). The crystallization behavior of the copolymers was analyzed by differential scanning calorimetry (DSC) and X-ray diffraction (XRD). The crystallization behavior of the H-shaped block copolymers demonstrated a PCL dominate crystallization. The self-assembly behavior of the copolymers was investigated in aqueous media. The hydrodynamic diameters of the copolymer micelles in aqueous solution were measured by dynamic light scattering (DLS). The morphology of the copolymer micelles was observed by atomic force microscopy (AFM) and transmission electron microscopy (TEM). The hydrodynamic diameters of spherical micelles declined gradually with the increase of the hydrophobic chain lengths of the copolymers. The critical micelle concentration (CMC) values were determined from fluorescence emission, and it was found that the CMCs decreased with an increase of PSt hydrophobic block lengths.

Keywords: atom transfer radical polymerization (ATRP), enzymatic ring-opening polymerization (eROP), amphiphilic block copolymer.

Introduction

An increased focus on amphiphilic block copolymers has taken place, owing to their superiority in industrial and biomedical applications such as biological engineering and drug delivery.[1-4] Some synthetic routes have been exploited to synthesize amphiphilic block copolymers, including living anionic polymerization,[5-7] cationic polymerization,[8-10] and the controlled/"living" radical polymerization and so forth.[11-13] Among these methods reported, living radical polymerization (LRP), which exemplifies stable free radical polymerization (SFRP),[14,15] atom transfer radical polymerization (ATRP),[16-18] and reversible addition-fragmentation transfer polymerization (RAFT),[19-21] has become preferred to others lying in its accurate control of molecular weight, polydispersity, and chain-end functionality. The combination of fundamentally different synthetic techniques, however, proved to be more suitable to the synthesis of block copolymers, which has motivated more researchers to synthesize various block copolymers by this strategy.

†To whom correspondence should be addressed.
E-mail: liyapeng@jlu.edu.cn

Biocatalysis in a non-natural environment has been recognized as an efficient route to products over the past years, attributed to the applicability to a wide scope of transformations of small organic functional molecules.[22] *In vitro* enzyme catalysis, as a new environmentally friendly methodology, has been expanded to the polymer synthesis and modification. The green biocatalyst enzyme is a promising alternative to the conventional chemical organometallic catalyst[23,24] because of its non-toxicity, recyclability, (enatio-, regio- and chemo-) selectivity, biocompatibility and ability to operate under mild conditions.[25,26] Now as polymer science advanced, biocatalytic approach has been employed in the design and synthesis of polymers with well-defined architectures, some of which are very difficult to achieve using conventional chemical catalysts.[27-29] Enzymatic polymerization methods, however, are adversary to the synthesis of functional polymers bearing special groups, which will narrow down their application on the synthesis of some functional polymers. To overcome the disadvantage, the development of mutually compatible chemo- and biocatalytic methods is required.

In recent years, enzymatic ring-opening polymerization (eROP) has attracted widespread attention because of high-efficiency, specificity and environmental protection.[30-32] Self-assembling micelles based on amphiphilic block copolymers have been receiving great interest, due to their special properties in application areas such as solubilizer, drug controlled release carrier, catalyzer and microelectronics.[33-35] As one of the "living"/controlled polymerization approaches, atom transfer radical polymerization (ATRP) is a flexible technique, which can be performed in high yield and in multiple solvents (including water), and also allows the preparation of well-defined polymers with narrow molecular weight distribution, predictable chain length, controlled microstructure and controlled architecture. As known to date, ATRP has been successfully employed to the synthesis of many macromolecules with predetermined architectures.[16-18] Chemoenzymatic method, which combines eROP with ATRP, provides a new strategy to synthesize amphiphilic block copolymers with controlled molecular weight, well-tailored architecture and precisely adjustable functionality owing to its integration of advantages of both polymerization techniques.[36,37] Since Andreas Heise *et al*. first reported the chemoenzymatic synthesis of AB-type diblock copolymer PCL-*b*-PSt via the combination of eROP of CL and ATRP of St,[38] more researchers have attempted to employ chemoenzyme-catalyzed routes to construct block copolymers. Armes and coworkers synthesized two bifunctional ATRP macroinitiators using Michael addition reaction, from which hydrophilic methacrylic monomers propagated via ATRP, to produce Y-shaped block copolymers.[39] Our group has reported the synthesis of block copolymers by chemoenzymatic method, such as AB-type block copolymers PCL-*b*-PSt, ABA-type block copolymers PSt-*b*-PCL-*b*-PSt, and the pentablock copolymers PHFMA-*b*-PCL-*b*-PEG-*b*-PCL-*b*-PHFMA and PSt-*b*-PCL-*b*-PEG-*b*-PCL-*b*-PSt.[40-42] Two pairs of building blocks were aligned along the same axle in a symmetry distribution, compared to traditional linear polymers, so the self-assembly of a H-shaped block copolymer into micelles in selective solvent (i.e. water) would exhibit more stable structures.

In this paper, we reported chemoenzymatic synthesis of H-shaped amphiphilic pentablock copolymers $(PSt)_2$-*b*-PCL-*b*-PEO-*b*-PCL-*b*-$(PSt)_2$ based on PEO, PCL, and PSt by combining eROP and ATRP (Figure 1), and afterwards considered the properties of block copolymers in aqueous solution, though we have studied the morphology of its analogues in organic solvent.[41,43] The resulting pentablock copolymers $(PSt)_2$-*b*-PCL-*b*-PEO-*b*-PCL-*b*-$(PSt)_2$ are especially interesting because PCL has features like crystallizability, lack of toxicity, printability, and good mechanical properties. On the other hand, the also crystallizable PEO has superior properties for being non-toxic, flexible, hydrophilic, weakly immunogenic, and biocompatible. In fact, the linear pentablock copolymers comprised of PSt, PEO, and PCL have been reported.[41] Nevertheless, no reports have been published on their analogous synthesis of H-shaped block copolymers $(PSt)_2$-*b*-PCL-*b*-PEO-*b*-PCL-*b*-$(PSt)_2$. The goal of this work is to further investigate

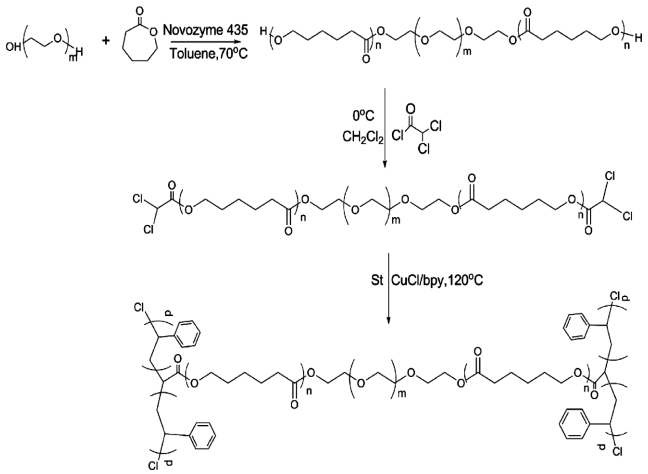

Figure 1. Synthetic route of H-shaped pentablock copolymers $(PSt)_2$-*b*-PCL-*b*-PEO-*b*-PCL-*b*-$(PSt)_2$.

the compatibility between eROP and ATRP. The H-shaped block copolymers can form micelles in aqueous solution, so the self-assembly behavior also makes these H-shaped block copolymers promising in polymer science as well as in biomedical and industrial application.

Experimental

Materials and Methods. Novozyme 435 (immobilized Candida Antarctica lipase B, specific activity 7000 PLU/g) was provided by Novozymes (Denmark). Dihydroxyl PEO (2000 Da) was purchased from FlukaChemical Co., and to desiccate water, exposed to vacuum at 80 °C for 24 h. Styrene (Beijing Chemical Co.) and ε-caprolactone (Aldrich Chemical Co.) were stirred over calcium hydride (CaH_2) overnight and distilled under vacuum before use. Copper (I) chloride (CuCl, Beijing Chemical Co.) was purified by precipitation from acetic acid to remove Cu^{2+}, filtrated and washed with ethanol, and then dried. 2,2-Bipyridine (Beijing Chemical Co.) and 2,2-dichloro acetyl chloride (DCAC, 99%) (Aldrich Chemical Co.) were used directly without further purification. Toluene (Tianjin Chemical Co.) and dichloromethane (Tianjin Chemical Co.) were dried with CaH_2 and distilled with argon protection. Triethylamine (Beijing Chemical Co.) was refluxed for 12 h in the presence of CaH_2 and distilled under vacuum. Tetrahydrofuran (Sinopharm Chemical Reagent Co., Ltd.) was dried with sodium and then distilled, when the liquid turned blue indicated by benzophenone. All the reagents used in this study were of analytic grade.

The monomer conversion was determined by gravimetric method. ^{1}H NMR spectra were performed with a Bruker ARX-500 NMR spectrometer of 500 MHz, with $CDCl_3$ as solvent and trimethylsilane (TMS) as internal standard. Molecular weights and molecular weight distributions were measured with a Waters 410 Gel permeation chromatography (GPC) apparatus equipped with a 10 μm Styragel HT6E column (300 mm × 7.8 mm), using THF as the eluent at a flow rate of 1 mL/min. A polystyrene calibration curve was used to calibrate the columns. The infrared spectra (IR) of polymers were recorded on a NICOLET Impact 410 at room temperature. Dried samples (20 mg) were mixed with 100 mg of dry KBr and pressed into disk (100 kg/cm^2). Differential scanning calorimetry (DSC) curves of the copolymers were recorded on Mettler Toledo Stare System DSC821e. The DSC measurements were performed on 3-6 mg samples under a nitrogen purge at a 10 °C/min scan rate. X-ray diffraction spectra (XRD) of the copolymers were recorded with Shimadazu XRD-6000 (CuKα $\lambda = 0.1546$ nm, 35 kV, 25 mA). Fluorescence emission spectra of copolymer aqueous solutions were obtained with Jobin Yvon Spex Fluorolog 3 fluorescence spectrophotometer. The average diameters and polydispersity of the copolymers were measured by dynamic laser scattering (DLS) at room temperature, using a laser light scattering spectrometer (BI-200SM) equipped with a laser source (514 nm) and a digital correlator (BI-9000AT). Atomic force microscopy (AFM) images were recorded on the commercial instrument (Digital Instrument, Nanoscope IIIa, Multimode) equipped with the microfabricated rectangle crystalsilicon cantilevers (Nanosensor) and operated in tapping mode at room temperature in air. A resonance frequency of approximately 365 kHz of the probe oscillation was chosen for all the topography images. The samples were prepared by dip-coating of freshly treated silicon wafer into a solution of the polymer micelles solution to form a monomolecular film. Transmission electron microscopy (TEM) studies were performed with a JEOL JEM 2010 instrument operated at an accelerator voltage of 200 kV. Micelle solution was dropped onto a carbon-coated copper grid, followed by the removal of excess sample with filter paper, and then air dried prior to measurements.

Synthesis of Block Copolymer HO-PCL-*b*-PEO-*b*-PCL-OH. Novozyme 435 (0.216 g, 10% w/w of the monomer weight) was dried over P_2O_5 in a vacuum desiccator (0.1 mm Hg, 25 °C, 24 h), then was transferred into a 50 mL dry and argon-filled vial, and the vial was tightly sealed with a rubber septum. The monomer caprolactone (2.156 g, 1.89×10^{-2} mol), the initiator PEO 2000 (0.378 g, 1.89×10^{-4} mol) and the solvent toluene (4.3 mL) were discharged into the reaction vial via an airtight syringe. The vial was immersed in oil bath stabilized at 70 °C while stirring for 4 h. Polymerization was terminated by pouring excess cold chloroform and removing the enzyme by filtration, and then washed several times with hot chloroform. The filtrate was concentrated by rotary evaporation, precipitated in methanol and dried in a vacuum oven. The yield was 85%.

Synthesis of Functional Macroinitiator $(Cl)_2$PCL-*b*-PEO-*b*-PCL$(Cl)_2$. The resulting HO-PCL-*b*-PEO-*b*-PCL-OH (1.2 g, 1×10^{-4} mol) was dissolved in 5 mL of dry dichloromethane contained in an around bottom flask and then cooled in an ice bath (0 °C). To this solution was added 1 mL (7.2×10^{-3} mol) of triethylamine with magnetic stirring and then DCAC (0.6 mL, 6.2×10^{-3} mol) in 5 mL of dichloromethane at a rate of about one drop every two seconds. The reaction mixture was main-

tained at 0 °C under stirring for 2 h and then raised to room temperature, which was allowed to stir for 22 h. The removal of precipitated byproduct was conducted through filtration. The obtained filtrate was subjected to rotary evaporation, yielding a concentrated solution, prior to precipitation in methanol. The precipitate was white solid which was collected after drying for 24 h under vacuum. Yield: 85%.

Synthesis of H-shaped Copolymer $(PSt)_2$-*b*-PCL-*b*-PEO-*b*-PCL-*b*-$(PSt)_2$. In a typical experiment, a dry flask equipped with a magnetic stirrer was charged with CuCl (0.018 g, 1.8×10^{-4} mol)), bpy (0.084 g, 5.4×10^{-4} mol), and macroinitiator (0.18 g, 1.5×10^{-5} mol). The reaction vial was sealed and degassed by performing three times freeze-pump-thaw cycles. Pre-degassed solvent toluene (2.4 mL) and monomer St (2.4 mL, 2.25×10^{-2} mol) by argon were introduced into the flask via an Ar-washed syringe. Subsequently, the reaction was initiated in a constant temperature oil bath of 120 °C. After 120 min, the reaction was rapidly quenched by exposure to air and immersed in an ice bath. The solution was diluted with chloroform. The copper was removed by passing over alumina column. The resulting crude polymer was precipitated in methanol and then dried under vacuum overnight, noted as copolymer 1. Polymerization and work-up of the samples (copolymer 2 and copolymer 3) were carried out as described above, where the reaction time was 210 and 480 min, respectively. Yield: 80%.

Formation of Copolymeric Micelles and Critical Micelle Concentration Determination. Formation of Copolymeric Micelles: The block copolymer $(PSt)_2$-*b*-PCL-*b*-PEO-*b*-PCL-*b*-$(PSt)_2$ (1 mg) was first dissolved in distilled THF (1 mL) at a concentration of 1 mg/mL, and sonicated for 10 min at room temperature, then distilled water was added dropwise to the copolymer/THF solution under vigorous stirring. The formation of micelles was indicated by the appearance of turbidity, which occurred when the water content reached 4, 3 and 1.5 wt % for this series of copolymers (copolymer 1, copolymer 2 and copolymer 3), respectively. To avoid the aggregation of individual micelles, more water was added until the volume reached about 20 mL, with the sample concentration of 0.05 mg/mL. The micelle mixture was further exposed to sonification for about 30 min at room temperature.

Critical Micelle Concentration Determination: A stock solution of pyrene was prepared by dissolving pyrene (5 mg, 25 μmol) in acetone (1 L) to form a 2.5×10^{-5} M solution. The pyrene solution (24 μL) was dropped via microliter syringe into empty vials, and the acetone was evaporated completely in a vacuum oven for 48 h. The $(PSt)_2$-*b*-PCL-*b*-PEO-*b*-PCL-*b*-$(PSt)_2$ micellar stock solution was serially diluted with deionized water starting with a concentration of 0.1 mg/mL down to 1.0×10^{-5} mg/mL. Each polymer solution (1 mL) was transferred into the pyrene-containing vial and stirred overnight. The final pyrene concentration in the polymer solutions reached 5×10^{-7} M, lower than the pyrene saturation concentration in water. Fluorescence measurements were performed by exciting samples at 335 nm, with excitation slit width of 3 nm and emission slit width of 1.5 nm. Emission wavelengths were scanned from 350 to 500 nm. The intensity ratio of I_1 (372 nm) to I_3 (383 nm) vibronic bands were plotted against the log of the concentration of each polymeric sample and the intersection of two regression lines calculated from the linear portions of the graphs represented the values of the critical micelle concentration (cmc).

Results and Discussion

PEO-initiated ROP of caprolactone catalyzed by Novozyme 435 was carried out at 70 °C in toluene (twice w/v of monomer). Water would compete with hydroxyl-capped PEO for initiation of lactones, as an effective initiator in the enzymatic ROP, resulting in carboxyl functionalized-PCL chains which were not functionalized with hydroxyl residue to provide macroinitiators for ATRP via further modification. Therefore to eliminate the negatively affected polymer structure caused by water initiation, it is of the utmost importance to dry reaction components thoroughly. A typical ^{1}H NMR spectrum of the resulting copolymer PCL-*b*-PEO-*b*-PCL was shown in Figure 2(a). Beside the dominant PCL signals b-f, the sharp singlet peak a, corresponding to the methylene protons of initiator PEO, could be discerned clearly at 3.61 ppm, which evidenced that PEO initiated eROP of CL. The GPC analysis of copolymer PCL-*b*-PEO-*b*-PCL showed a unimodal and symmetrical trace in Figure 3(a). GPC-determined molecular weight (M_n) was 16600 g/mol and polydispersity was 1.49, respectively, as listed in Table 1. The block copolymer PCL-*b*-PEO-*b*-PCL was converted to tetrafunctional macroinitiator by its esterification with DCAC. To keep the polymer chains intact, the reaction was conducted at a freezing condition (0 °C) in purified CH_2Cl_2 in the presence of TEA, where TEA acted as a catalyst, absorbed HCl from the solution to generate a precipitate of quaternary ammonium halide $(CH_3CH_2)_3NH^+Cl$ and prompted the esterification.

Figure 2(b) showed a typical ^{1}H NMR spectrum of the mac-

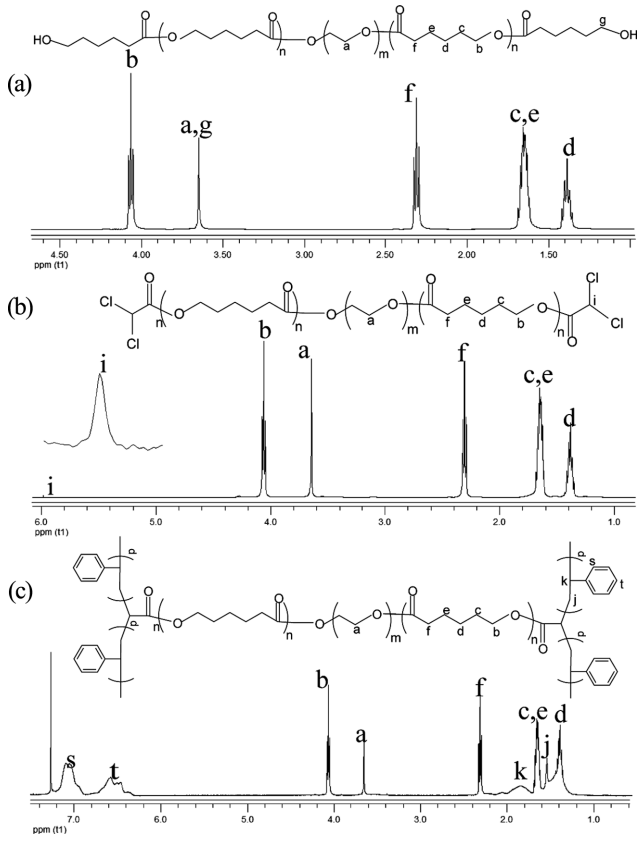

Figure 2. ^{1}H NMR spectra of the block copolymers: (a) PCL-*b*-PEO-*b*-PCL; (b) $(Cl)_2$PCL-*b*-PEO-*b*-PCL$(Cl)_2$; (c) $(PSt)_2$-*b*-PCL-*b*-PEO-*b*-PCL-*b*-$(PSt)_2$ (H-copolymer).

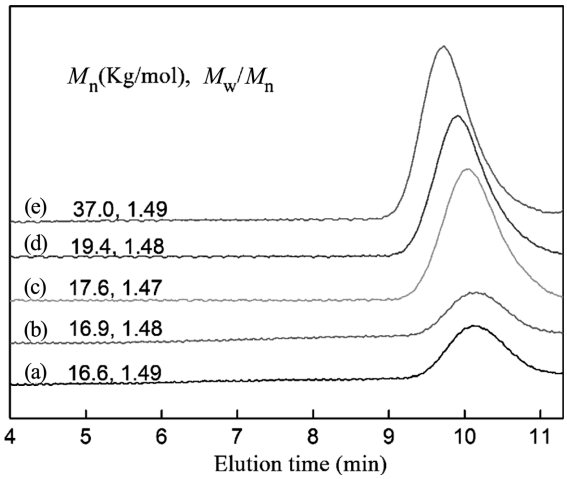

Figure 3. GPC spectra of the block copolymers: (a) PCL-*b*-PEO-*b*-PCL; (b) $(Cl)_2$PCL-*b*-PEO-*b*-PCL$(Cl)_2$; (c) H-copolymer 1; (d) H-copolymer 2; (e) H-copolymer 3.

roinitiator, where all characteristic peaks belonging to PCL-*b*-PEO-*b*-PCL could be identified. The appearance of resonance at 5.95 ppm could be assigned to the -CH- protons adjacent to the active chloride, indicating that the 2,2-dichloro acetyl group was attached to the PCL chain end. The intensity ratio of a to i was up to 90:0.5, which demonstrated an extremely high substitution efficiency of the terminal hydroxyl groups by 2,2-dichloro acetyl group. It can be seen from Table 1, the number-average molecular weight (M_n) was slightly higher in comparison with PCL-*b*-PEO-*b*-PCL, however, the value of polydispersity after the modification of end group dwindled to lower than those of the starting PCL. This could be attributed to inevitable fractionation of the macroinitiator during the course of precipitation after esterification.

To construct the H-shaped architectures was the premise for the successful synthesis of H-shaped block copolymers, so verification of the existence of two initiating centers in the same carbon [-$CH(Cl)_2$] was the essence of the experiment, which had been discussed in detail as previous works reported.[44] Figure 2(c) showed a typical ^{1}H NMR spectrum of the H-shaped copolymer. As can be seen in Figure 2(c), apart from the proton signals of $(Cl)_2$PCL-*b*-PEO-*b*-PCL$(Cl)_2$, the ones at about 6.3-7.3 ppm were attributed to the s and t protons of the benzene ring of PSt block. In addition, characteristic peaks

Table 1. Results of PCL, Macroinitiator and H-shaped Copolymers

	$[M]_0/[I]_0$	Time (min)	Monomer conversion (%)[b]	$M_{n,th}$ (g/mol)[c]	$M_{n,NMR}$ (g/mol)[a]	$M_{n,GPC}$ (g/mol)[d]	M_w/M_n[d]	Carboxyl terminal chains (mol%)[a]	Degree of end functionalization (mol%)
PCL	30/1		90	12300	12000	16600	1.49	<2	
Macroinitiator						16900	1.48		>98
H-Copolymer 1	1500/1	120	9.2	27200	26200	17600	1.47		
H-Copolymer 2	1500/1	210	12.9	33600	33000	19400	1.48		
H-Copolymer 3	1500/1	480	46.3	53500	49100	37000	1.49		

[a]Determined by ^{1}H NMR analysis. [b]The conversion was determined gravimetrically. [c]The theoretical molecular weights ($M_{n,th}$) calculated from the ratio of the monomer to the initiator $[M]_0/[I]_0$ and the monomer conversion. $M_{n,th} = ([M]_0/[I]_0) \times M_{monomer} \times$con.-% + $M_{n(macro)initiator}$. [d]Determined by GPC measurements.

belonging to methylene and methine protons of PSt block were observed at 1.45 and 1.84 ppm, respectively, indicating that PSt chains were grown from ATRP initiator site successfully. Typical GPC trace of H-shaped block copolymer 1 was shown in Figure 3(c) (other samples were also shown in Figure 3, as d and e, respectively), revealing a monomodal and quite symmetric elution peak. In comparison with that of $(Cl)_2$PCL-*b*-PEO-*b*-PCL$(Cl)_2$ macroinitiator, GPC trace of H-shaped copolymers exhibited a significant shift to higher M_W region, with number-average molecular weight of 17600 g/mol and polydispersity of 1.47. GPC analysis further confirmed the successful synthesis of the H-shaped copolymer. There were some inconsistency between $M_{n,NMR}$ and $M_{n,GPC}$, because GPC used monodisperse polystyrene as standard.

Figure 4 showed the IR spectra of PCL, macroinitiator, and H-shaped block copolymer. For PCL-*b*-PEO-*b*-PCL, new characteristic peaks appeared in the wavenumber region of 1732 cm^{-1}, which could be assigned to ester carbonyl group of PCL block, apart from ones at 1105 cm^{-1} belonging to stretching vibration of ether bond from initiator moiety PEO. After the polymerization of styrene, besides the PCL peaks, the occurrence of absorption bands at the wavenumbers of about 3035, 1449, 689 cm^{-1} were ascribed to the presence of aromatic ring of PSt blocks.

The results of the ^{1}H NMR, GPC and IR analyses confirmed that the H-shaped amphiphilic block copolymer was successfully synthesized using eROP and ATRP.

DSC was carried out to investigate the melting and crystallization behaviors of the H-shaped pentablock copolymers 1, copolymers 2 and copolymers 3 with different chain lengths. DSC analysis was performed in the range from -70 to 110 °C at a heating rate of 10 °C/min under nitrogen. To minimize the effect of crystallization history, we evaluated the thermal properties based on the second thermal scan. Figure 5(A) and Figure 5(B) showed DSC curves of copolymers during the cooling process and those of copolymers during the second heating process respectively. It can be easily seen that a single peak was observed in both DSC curves. As observed in Figure 5(B), the value of melting point of copolymers was close to that of their counterpart, PCL homopolymers, as reported in literatures.[45] This result revealed that the crystallization ability of PCL block was not affected substantially, while PEO block was unexpectedly unable to rearrange into crystalline array,

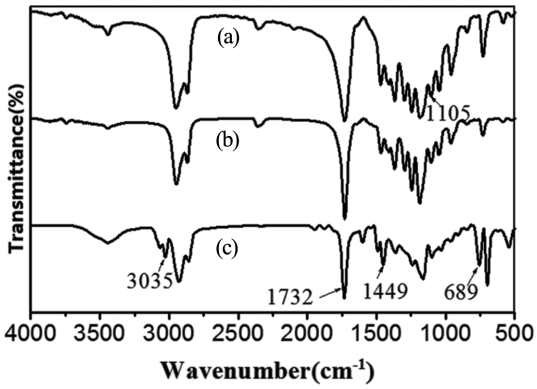

Figure 4. IR spectra of PCL-*b*-PEO-*b*-PCL (a); $(Cl)_2$-PCL-*b*-PEO-*b*-PCL-$(Cl)_2$ (b); $(PSt)_2$-*b*-PCL-*b*-PEO-*b*-PCL-*b*-$(PSt)_2$ (c).

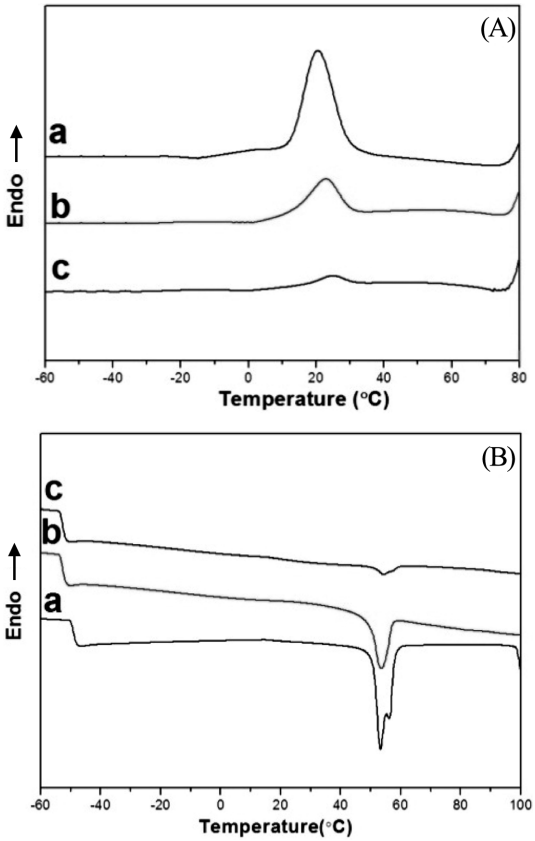

Figure 5. DSC curves of the H-shaped copolymers during the cooling process (A); second heating process (B) a. H-copolymer 1, b. H-copolymer 2, c. H-copolymer 3.

Table 2. DSC Results for the H-shaped Block Copolymers

Sample	T_c (°C)	T_m (°C)	(ΔH_m) (J/g)	X_c (%)[a]
Copolymer 1	18.19	53.25	40.64	30.1
Copolymer 2	20.23	55.37	28.90	21.4
Copolymer 3	21.74	56.93	12.37	9.2

[a] $X_c = (\Delta H_m/\Delta H_m^*) \times 100\%$, and ΔH_m^* means theoretical value of crystallization enthalpy of poly(ε-caprolactone), 135 J/g.

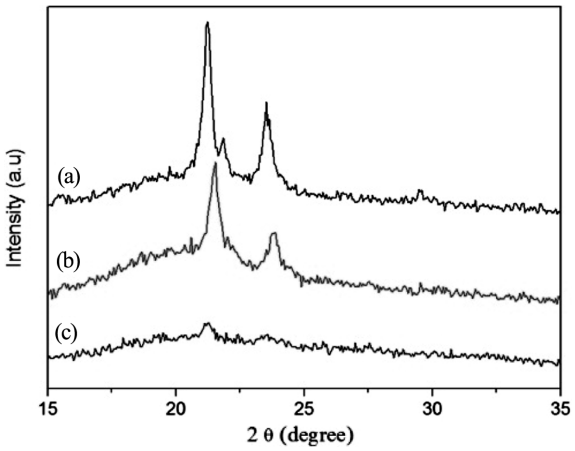

Figure 6. XRD spectra of the H-shaped copolymers: (a) H-copolymer 1; (b) H-copolymer 2; (c) H-copolymer 3.

attributed largely to its shorter block length relative to PCL block. As shown in Table 2, the relative crystallinity of copolymer was lowered gradually down to 9.2% (copolymer 3) from 30.1% (copolymer 1), since inhibition of the crystallization of PCL units caused by amorphous PSt block enhanced, as the amount of non-crystallizable styrene monomer increased in the molecular chain. DSC analysis further confirmed that H-shaped copolymers with different block lengths of PSt could be prepared by varying reaction time during ATRP of styrene, crucial to obtain materials with easily-controlled crystallization behavior.

In order to further investigate the crystallization of the H-shaped pentablock copolymers, the copolymers were characterized by XRD, as indicated in Figure 6. As can be seen

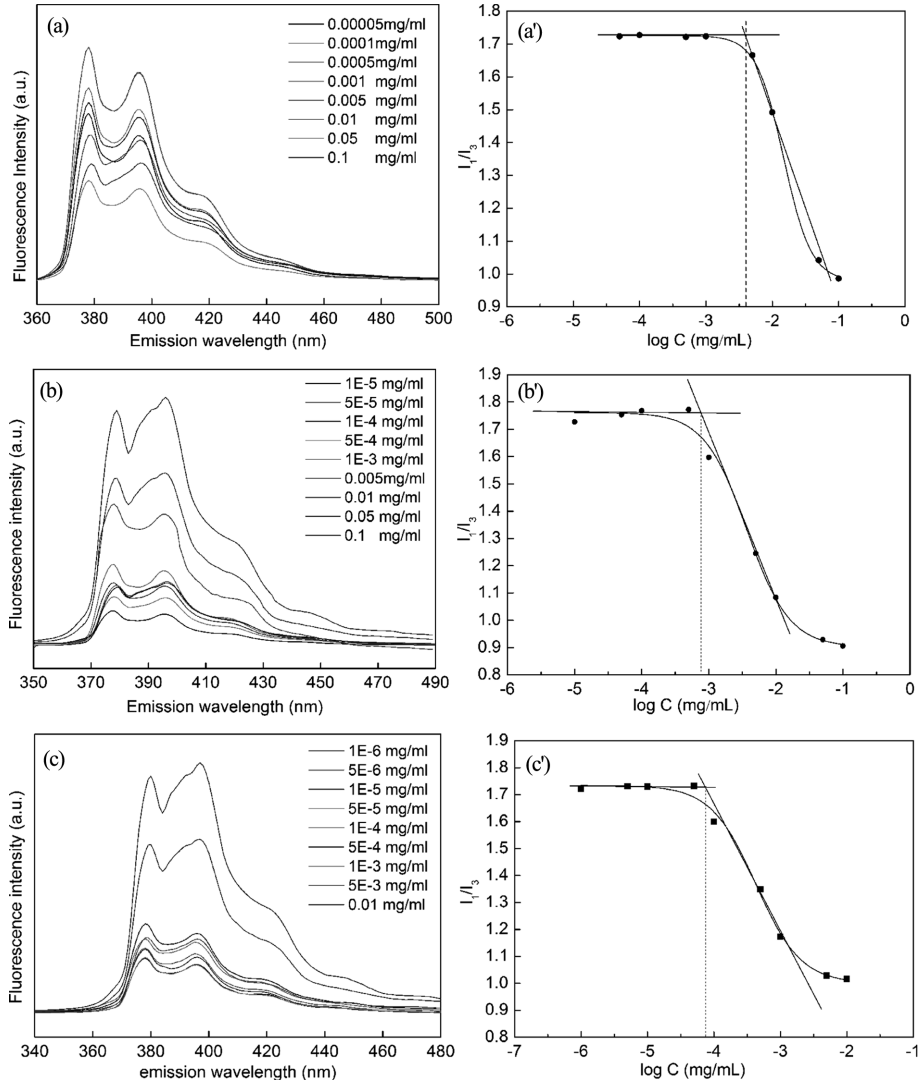

Figure 7. Fluorescence emission spectra of H-shaped copolymer aq. solutions at different concentrations and plot of I_1/I_3 against the log of different concentrations: (a), (a') H-copolymer 1; (b), (b') H-copolymer 2; (c), (c') H-copolymer 3.

from Figure 6(a) and 6(b), copolymer 1 and copolymer 2 displayed obvious reflections, indexed to (110) and (200). The crystal plane distance (*d*) of the two reflections were 0.41 and 0.37 nm, respectively. With the increase of PSt chains, the relative intensities of the diffraction peaks decreased gradually, even disappeared for copolymer 3 indicating a completely amorphous state, but no apparent shift in the positions of diffraction peaks could be observed. There was a weak peak at $2\theta = 29.5^{o}$, which could be ascribed to PEO crystallization. PEO block, however, was shorter compared with PCL block, leading to a larger reduce on crystallization ability for PEO block than PCL block. The crystallization behavior of the H-shaped block copolymers demonstrated a PCL-dominated crystallization.

The fluorescence emission spectra of pyrene probe at various concentrations of aqueous solution of the H-shaped pentablock copolymers were shown in Figure 7((a), (b) and (c) for copolymer 1, copolymer 2 and copolymer 3). The critical micelle concentrations (CMC) of copolymer 1, copolymer 2 and copolymer 3 were 0.005, 1.71×10^{-3} and 2.24×10^{-4} mg/mL, lower than the values of their linear block analogues with similar molecular weight.[42] It can be found that with an increase of PSt hydrophobic block length, the CMCs were decreased, consistent with the phenomenon that less water was needed for the micelles formation of copolymers bearing less hydrophobic unit, suggesting an enforced resistance to dilution after entering physiological environment. The explanation for this finding was that the aggregation of hydrophobic fractions occurred more easily, when block copolymers were comprised of more hydrophobic unit.

To study the size and size distribution of the H-shaped pentablock copolymer micelles, the copolymer micelle solutions were characterized using DLS, as illustrated in Figure 8. Dynamic light-scattering measurement of the polymer micelle solutions revealed that the average hydrodynamic diameters of copolymer 1, copolymer 2 and copolymer 3 were 330.2, 313.0 and 255.3 nm, respectively, with the corresponding polydispersity indexes of 0.243, 0.266 and 0.141. Of more importance, DLS analysis showed that the size of polymeric micelles declined, as the hydrophobic block length (i.e. PCL and PSt) extended, because hydrophobic modules, which served as inner core of core-shell micelles, aggregated more compactly in response to an increase of hydrophobic interaction arising from the introduction of more monomers (styrene) with low polarity.

To observe the self-assembly morphology, we used tapping mode AFM and TEM to study the H-shaped block copolymer aggregates in the dry state. Figure 9 and Figure 10 separately showed typical AFM and TEM images of the polymeric aggregates prepared from aqueous solutions, where the samples were exposed to high vacuum, and we could find that spherical micelles formed in the samples. The average diameters of the spherical nanoparticles of copolymer 1, copolymer 2 and copolymer 3 were 182, 165 and 133 nm. The main reason of formation of spheroidal structure might be the relatively high density and a longer hydrophobic chain on the H-shaped block copolymers, and in order to obtain a more stable structure, the construction of micelles was necessary to increase the proportion of hydrophobic blocks. The size of micelles determined by DLS analysis seemed larger than those by AFM and TEM, primarily due to that the micelles were swollen in solutions during the DLS measurements, whereas AFM and TEM showed the diameters of the dried aggregates. The variation between polymeric micelles prior to drying and ones in water-free state was most distinct for copolymer 1, due to its highest proportion of PEO segment in the molecular chain which interweaved with its surrounding water molecules and contributed to a noticeable increase in size of polymer aggregates.

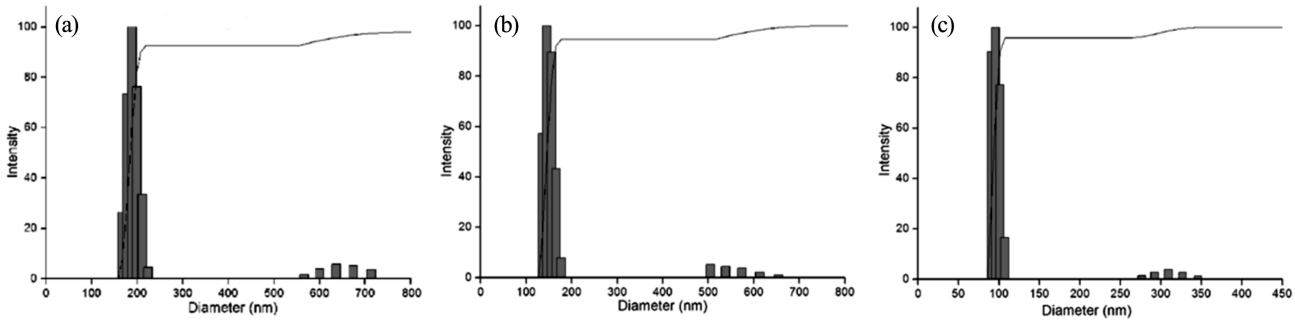

Figure 8. Lognormal size distribution of micelles formed by the H-shaped copolymers in aqueous environment: (a) H-copolymer 1; (b) H-copolymer 2; (c) H-copolymer 3.

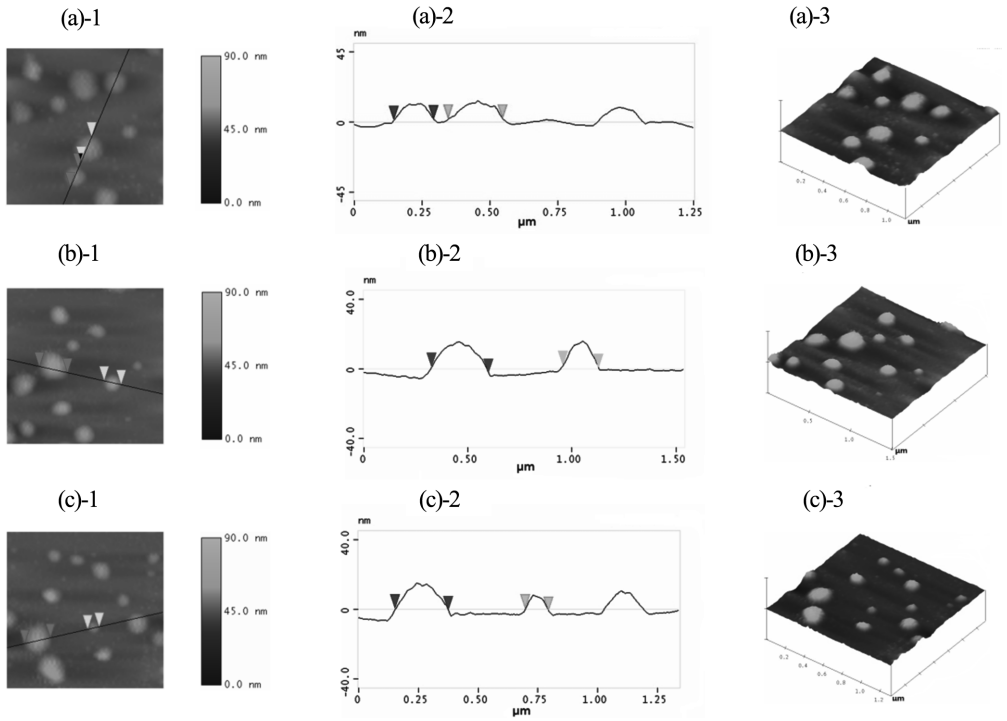

Figure 9. AFM images of the H-shaped copolymers: (a) H-copolymer 1; (b) H-copolymer 2; (c) H-copolymer 3.

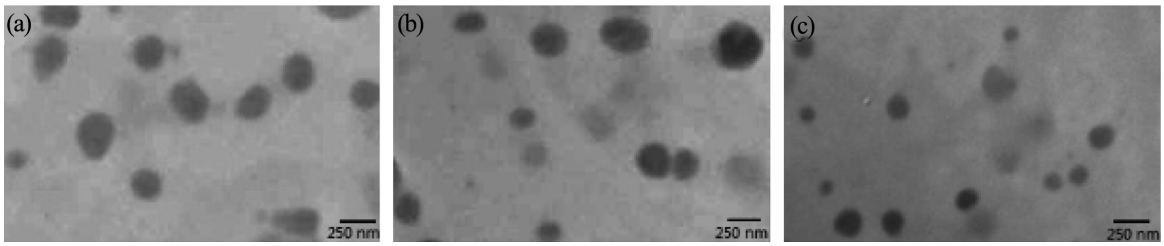

Figure 10. TEM images of the H-shaped copolymers: (a) H-copolymer 1; (b) H-copolymer 2; (c) H-copolymer 3.

Conclusions

The H-shaped pentablock copolymer $(PSt)_2$-*b*-PCL-*b*-PEO-*b*-PCL-*b*-$(PSt)_2$ was synthesized via dichloropolyester, initially synthesized by eROP of CL, as a macroinitiator for the ATRP of styrene. The structures, molecular weight and molecular weight distribution of all the polymer products were confirmed by NMR, FTIR and GPC measurements. We systemically studied the influence of the ratios of the constituent blocks (PCL : PSt) on the properties of the copolymers, such as crystallization behaviors and the self-assembling behavior in aqueous solution. The finding is that those copolymers demonstrated a PCL dominant crystallization. These H-shaped block copolymer aggregates examined by AFM and TEM showed spherical morphologies. Due to their unique properties, they have great potential in drug delivery and bio-engineering.

References

1. C. S. Cho, Y. I. Jeong, S. H. Kim, J. W. Nah, Y. M. Lee, I. K. Kang, and Y. K. Sung, *Polymer(Korea),* **7**, 203 (1999).
2. M. Prabaharan, J. J. Grailer, S. Pilla, D. A. Steeber, and S. Q. Gong, *Biomaterials*, **30**, 6065 (2009).
3. A. Blanazs, S. P. Armes, and A. J. Ryan, *Macromol. Rapid Commun.*, **30**, 267 (2009).
4. Y. J. Kim, Y. K. Sung, A. Z. Pial, and S. W. Kim, *Polymer(Korea),* **5**, 214 (1997).
5. E. Ruckenstein and H. M. Zhang, *Macromolecules*, **31**, 9127 (1998).
6. A. Hirao, M. Hayashi, and N. Haraguchi, *Macromol. Rapid Commun.*, **21**, 1171 (2000).

7. A. Hirao, T. Higashihara, and K. Inoue, *Macromolecules,* **41**, 3579 (2008).
8. T. Yoshida, K I. Seno, S. Kanaoka, and S. Aoshima, *J. Polym. Sci. Part A: Polym. Chem.*, **43**, 1155 (2005).
9. S. Aoshima, S. Sugihara, M. Shibayama, and S. Kanaoka, *Macromol. Symp.*, **215**, 151 (2004).
10. S. Aoshima and S. Sugihara, *J. Polym. Sci. Part A: Polym. Chem.,* **38**, 3962 (2000).
11. M. F. Cunningham, *Prog. Polym. Sci.*, **33**, 365 (2008).
12. K. Matyjaszewski and J. Spanswick, *Materialstoday*, **8**, 26 (2005).
13. J. Y. Lee, J. H. Kim, M. J. Kim, and M. K. Jin, *Polymer(Korea)*, **7**, 229 (1999).
14. P. Gopalan, Y. M. Zhang, X. F. Li, U. Wiesner, and C. K. Ober, *Macromolecules*, **36**, 3357 (2003).
15. A. J. Pasquale and T. E. Long, *J. Polym. Sci. Part A: Polym. Chem.,* **39**, 216 (2001).
16. V. Coessens, T. Pintauer, and K. Matyjaszewski, *Prog. Polym. Sci.*, **26**, 337 (2001).
17. N. V. Tsarevsky and K. Matyjaszewski, *Chem. Rev.*, **107**, 2270 (2007).
18. M. Licciardi, Y. Tang, N. C. Billingham, and S. P. Armes, *Biomacromolecules,* **6**, 1085 (2005).
19. A. W. York, S. E. Kirkland, and C. L. McCormick, *Adv. Drug Deliver. Rev.*, **60**, 1018 (2008).
20. C. Z. Li and B. C. Benicewicz, *Macromolecules*, **38**, 5929 (2005).
21. A. B. Lowe and C. L. McCormick, *Prog. Polym. Sci*., **3**, 283 (2007).
22. A. WellsF, *Org. Process. Res. Dev.*, **10**, 678 (2006).
23. J. T. Scarpello, D. Nair, L. M. Freitas dos Santos, L. S. White, and A. G. Livingston, *J. Membr. Sci.*, **203**, 71 (2002).
24. C. Torque, H. Bricout, F. Hapiot, and E. Monflier, *Tetrahedron,* **60**, 6487 (2004).
25. F. López-Gallego, L. Betancor, A. Hidalgo, C. Mateo, J. M. Guisán, and R. Fernández-Lafuente, *Biotechnol.*, **111**, 219 (2004).
26. J. B. Van Beilen and Z. Li, *Curr. Opin. Biotechnol.*, **13**, 338 (2002).
27. Y. Murakami, R. Hoshi, and A. Hirata, *J. Mol. Catal. B: Enzym.*, **22**, 79 (2003).
28. A. E. Ivanov, E. Edink, A. Kumar, I. Y. Galaev, A. F. Arendsen, A. Bruggink, and B. Mattiasson, *Biotechnol. Progr.*, **19**, 1167 (2003).
29. R. Konwarh, D. Kalita, C. Mahanta, M. Mandal, and N. Karak, *Appl. Microbiol. Biotechnol.*, **87**, 1983 (2010).
30. A. C. Albertsson and R. K. Srivastava, *Adv. Drug Deliver. Rev.*, **60**, 1077 (2008).
31. A. Makino and S. Kobayashi, *J. Polym. Sci. Part A: Polym. Chem.*, **48**, 1251 (2010).
32. X. H. Yu, R. X. Zhuo, J. Feng, and J. Liao, *Eur. Polym. J*., **40,** 2445 (2004).
33. D. Le Garrec, S. Gori, L. Luo, D. Lessard, D. C. Smith, M. A. Yessine, M. Ranger, and J. C. Leroux, *J. Control. Release*, **99**, 83 (2004).
34. E. K. Park, S. Y. Kim, S. B. Lee, and Y. M. Lee, *J. Control. Release*, **109**, 158 (2005).
35. R. K. O'Reilly, C. J. Hawker, and K. L. Wooley, *Chem. Soc. Rev.*, **35**, 1068 (2006).
36. S. Villarroya, J. X. Zhou, K. J. Thurecht, and S. M. Howdle, *Macromolecules*, **39**, 9080 (2006).
37. M. De Geus, A. R. A. Palmans, C. J. Duxbury, S. Villarroya, S. M. Howdle, and A. Heise, *Polymer Biocatalysis and Biomaterials II*, **14**, 216 (2008).
38. U. Meyer, A. R. A. Palmans, T. Loontjens, and A. Heise, *Macromolecules*, **35**, 2873 (2002).
39. Y. L. Cai, Y. Q. Tang, and S. P. Armes, *Macromolecules*, **37**, 9728 (2004).
40. K. Sha, L. Qin, D. S. Li, X. T. Liu, and J. Y. Wang, *Polym. Bull.,* **54**, 1 (2005).
41. K. Sha, D. S. Li, Y. P. Li, B. Zhang, and J. Y. Wang, *Macromolecules*, **41**, 361 (2008).
42. W. Wang, Y. P. Li, Y. L. Zhao, B. Zhang, and J. Y. Wang, *Acta Polym. Sin.*, **2**, 199 (2010).
43. B. Zhang, Y. P. Li, J. H. Sun, S. W. Wang, Y. L. Zhao, and Z. Y. Wu, *Polym. Int*., **58**, 752 (2009).
44. D. Wang, B. Zhang, Y. P. Li, and J. H. Sun, *Chem. J. Chinese. U*., **29**, 1479 (2008).
45. B. Zhang, Y. P. Li, P. Ai, Z. P. Sa, Y. L. Zhao, M. Li, D. Wang, and K. Sha, *J. Polym. Sci. Part A: Polym. Chem*., **47**, 5509 (2009).